

# Blind Decoding of Multiple Description Codes over OFDM Systems via Sequential Monte Carlo

**Zigang Yang**

*Texas Instruments Inc, 12500 TI Boulevard Dallas, MS 8653 Dallas, TX 75243, USA*  
*Email: zigang@ti.com*

**Dong Guo**

*Department of Electrical Engineering, Columbia University, New York, NY 10027, USA*  
*Email: guodong@ee.columbia.edu*

**Xiaodong Wang**

*Department of Electrical Engineering, Columbia University, New York, NY 10027, USA*  
*Email: wangx@ee.columbia.edu*

*Received 1 May 2004; Revised 20 December 2004*

We consider the problem of transmitting a continuous source through an OFDM system. Multiple description scalar quantization (MDSQ) is applied to the source signal, resulting in two correlated source descriptions. The two descriptions are then OFDM modulated and transmitted through two parallel frequency-selective fading channels. At the receiver, a blind turbo receiver is developed for joint OFDM demodulation and MDSQ decoding. Transformation of the extrinsic information of the two descriptions are exchanged between each other to improve system performance. A blind soft-input soft-output OFDM detector is developed, which is based on the techniques of importance sampling and resampling. Such a detector is capable of exchanging the so-called extrinsic information with the other component in the above turbo receiver, and successively improving the overall receiver performance. Finally, we also treat channel-coded systems, and a novel blind turbo receiver is developed for joint demodulation, channel decoding, and MDSQ source decoding.

**Keywords and phrases:** multiple description codes, OFDM, frequency-selective fading, sequential Monte Carlo, turbo receiver.

## 1. INTRODUCTION

Multiple description scalar quantization (MDSQ) is a source coding technique that can exploit diversity communication systems to overcome channel impairments. An MDSQ encoder generates multiple descriptions for a source and sends them over different channels provided by the diversity systems. At the receiver, when all descriptions are received correctly, a high-quality reconstruction is possible. In the event of failure of one or more of the channels, the reconstruction would still be of acceptable quality.

The problem of designing multiple description scalar quantizers is addressed in [1, 2], where a theoretical performance bound is derived in [1] and practical design methods are given in [2, 3]. Conventionally, MDSQ has been

investigated only from the perspective of transmission over erasure channels, that is, channels which either transmit noiselessly or fail completely [1, 2, 4]. Recently, it was shown in [5] that an MDSQ can be used effectively for communication over slow-fading channels. In that system, a threshold on the channel fade values is used to determine the acceptability of the received description. The signal received from the bad connection is not utilized at the receiver.

In this paper, we propose an iterative MDSQ decoder for communication over fading channels, where the extrinsic information of the descriptions is exchanged with each other by exploiting the correlation between the two descriptions. Although the MDSQ coding scheme provided in [2] is optimized with the constraint of erasure channels, it provides very nice correlation property between different descriptions. Therefore, the same MDSQ scheme will be applied to the continuous fading environment considered in this paper [6, 7, 8].

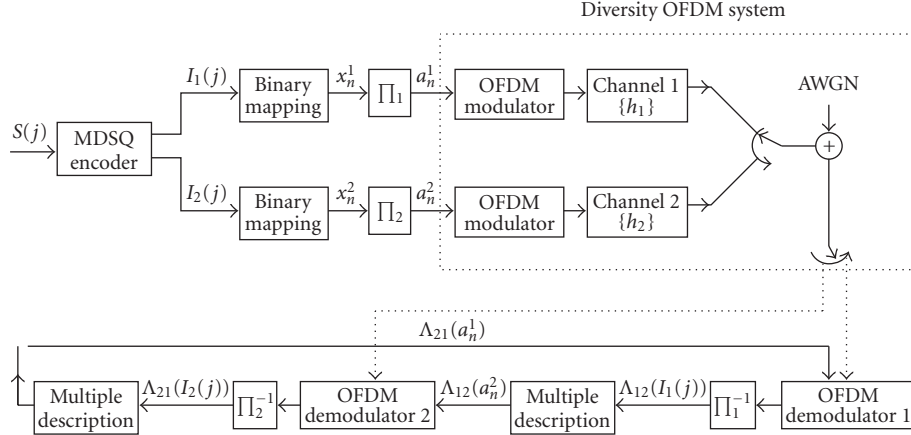


FIGURE 1: Continuous source transmitted through a diversity OFDM system with MDSQ.

Providing high-data-rate transmission is a key objective for modern communication systems. Recently, orthogonal frequency-division multiplexing (OFDM) has received a considerable amount of interests for high-rate wireless communications. Because OFDM increases the symbol duration and transmitting data in parallel, it has become one of the most effective modulation techniques for combating multipath delay spread over mobile wireless channels.

In this paper, we consider the problem of transmitting a continuous source through an OFDM system over parallel frequency-selective fading channels. The source signals are quantized and encoded by an MDSQ, resulting in two correlated descriptions. These two descriptions are then modulated by OFDM and sent through two parallel fading channels. At the receiver, a blind turbo receiver is developed for joint OFDM demodulation and MDSQ decoding. Transformation of the extrinsic information of the two descriptions are exchanged between each other to improve system performance. The transformation is in terms of a transformation matrix which describes the correlation between the two descriptions. Another novelty in this paper is the derivation of a blind detector based on a Bayesian formulation and sequential Monte Carlo (SMC) techniques for the differentially encoded OFDM system. Being soft-input and soft-output in nature, the proposed SMC detector is capable of exchanging the so-called extrinsic information with the other component in the above turbo receiver, successively improving the overall receiver performance.

For a practical communication system, channel coding is usually applied to improve the reliability of the system. In this paper, we also treat a channel-coded OFDM system, where each stream of the source description is channel encoded and then OFDM modulated before being sent to the channel. At the receiver, a novel blind turbo receiver is developed for joint demodulation, channel decoding, and source decoding.

The rest of this paper is organized as follows. In Section 2, the diversity of an OFDM system with an MDSQ encoder is described. In Section 3, the turbo receiver is discussed for

the MDSQ encoded OFDM system. In Section 4, we develop an SMC algorithm for blind symbol detection of OFDM systems. A turbo receiver for a channel-coded OFDM system is derived in Section 5. Simulation results are provided in Section 6, and a brief summary is given in Section 7.

## 2. SYSTEM DESCRIPTION

We consider transmitting a continuous source through a diversity OFDM system. The diversity of an OFDM system is made up of two  $N$ -subcarrier OFDM systems, signalling through two parallel frequency-selective fading channels. Such a parallel channel structure was first introduced in [9]. A block diagram of the system is shown in Figure 1. A sequence of continuous sources  $\{S(j)\}$  is encoded by a multiple description scalar quantizer (MDSQ), resulting in two sets of equal-length indices  $\{(I_1(j), I_2(j))\}$ , where  $j$  denotes the sequence order. The detailed MDSQ encoder will be discussed in Section 2.1. These indices can be further described in a binary sequence  $\{(x_n^1, x_n^2)\}$  with the order denoted by  $n$ . The bit interleavers  $\pi_1$  and  $\pi_2$  are used to reduce the influence of error bursts at the input of the MDSQ decoder. After the interleaved bits  $\{a_n^1\}$ ,  $\{a_n^2\}$  are modulated by OFDM, we use the parallel concatenated transmission scheme shown in Figure 1; that is, one description of the source is transmitted through one channel and the other description is transmitted through another channel. At the receiver, the OFDM demodulators, which will be discussed in Section 4, generate soft information, which is then exchanged between the two OFDM detectors in the form of *a priori* probabilities of the information symbols. Next, we will focus on the structure of the MDSQ encoder and the diversity OFDM system.

### 2.1. Multiple description scalar quantizer

#### 2.1.1. Multiple description scalar quantizer for diversity on/off channels

The multiple description scalar quantizer (MDSQ) is a scalar quantizer designed for the channel model illustrated

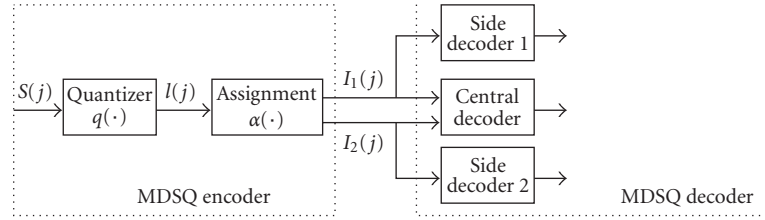
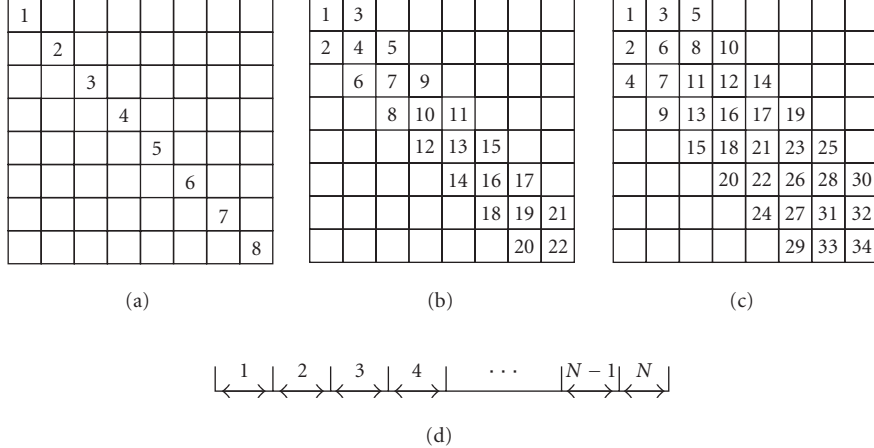


FIGURE 2: Conventional MDSQ in a diversity system.

FIGURE 3: MDSQ index assignment for  $R = 3$ . A quantized source sample  $l(j) \in \{1, 2, \dots, N\}$  is mapped to a pair of indices  $(I_1(j), I_2(j)) \subset \mathcal{C}$  composed of its associated row and column determined by the assignment  $\alpha(\cdot)$ . (a) Assignment with  $N = 8$ . (b) Assignment with  $N = 22$ . (c) Assignment with  $N = 34$ . (d) Quantizer.

in Figure 2. The channel model consists of two channels that connect the source to the destination. Either channel may be broken or lossless at any time. The encoder of an MDSQ sends information over each channel at a rate of  $R$  bits/sample. Based on the decoder structure shown in Figure 2, the objective is to design an MDSQ encoder so as to minimize the average distortion when both channels are lossless (center distortion), subject to a constraint on the average distortion when only one channel is lossless (side distortion).

Next, we give a brief summary of the MDSQ design presented in [2]. Denote an index set  $\mathcal{J} = \{1, 2, \dots, M\}$ , where  $M = 2^R$ . Let  $\mathcal{C} \subset \mathcal{J} \times \mathcal{J}$  and  $|\mathcal{C}| = N \leq M^2$ . The MDSQ encoder consists of an  $N$ -level quantizer  $q(\cdot) : \mathcal{R} \rightarrow \{1, 2, \dots, N\}$  followed by index assignment  $\alpha(\cdot) : \{1, 2, \dots, N\} \rightarrow \mathcal{C}$ . Note that  $N$  is both the size of  $\mathcal{C}$  and the number of the quantization levels. Specifically, a source sample  $S(j)$  is mapped to an index  $l(j) \in \{1, 2, \dots, N\}$  by the quantizer  $q(\cdot)$ , which is further mapped to a pair of indices  $(I_1(j), I_2(j)) \subset \mathcal{C}$  by the assignment  $\alpha(\cdot)$ .

Assume a uniform quantizer. The main issue in MDSQ design is the choice of the set  $\mathcal{C}$ , and the index assignment  $\alpha(\cdot)$ . Following [2], an example of good assignment

for  $R = 3$  bits/sample is illustrated in Figure 3. We assume that the cells of a quantizer are numbered  $1, 2, \dots, N$ , in increasing order from left to right as shown in Figure 3d. Intuitively, with a larger set  $\mathcal{C}$ , center distortion will be improved at the expense of degraded side distortion. With the same size of the set  $\mathcal{C}$ , the center distortion is fixed, and a diagonal-like assignment is preferred to minimize the side distortion.

### 2.1.2. Multiple description scalar quantizer for diversity fading channels

Although MDSQ was originally designed for diversity erasure channels, it provides a possible solution that combines source coding and channel coding to exploit the diversity provided by communication systems. Next, we consider the application of MDSQ techniques in diversity fading channels.

At the transmitter, we apply the MDSQ encoder as the conventional (cf. Figure 2). For each continuous source  $S(j)$ , a pair of indices  $(I_1(j), I_2(j))$  is generated by the MDSQ, and is further mapped to binary bits  $\{x_n^1, x_n^2\}_{n=(j-1)R+1}^{jR}$ . Recall that  $R$  denotes the bit-length of each description. At the receiver,

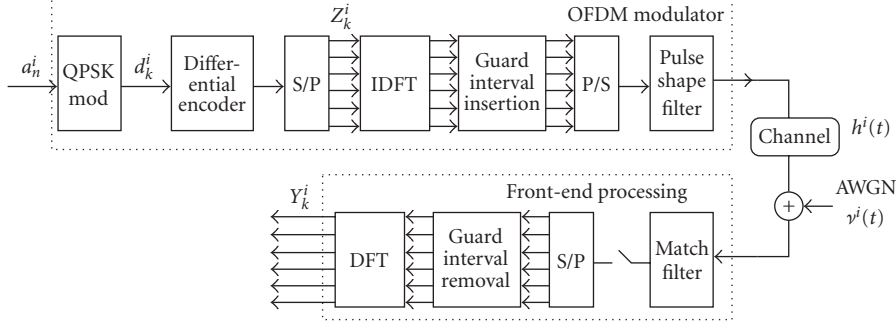


FIGURE 4: Block diagram of a baseband OFDM system.

instead of using the side decoder and central decoder, a soft MDSQ decoder is employed for MDSQ over fading channels. It is assumed that a soft demodulator is available at the receiver, which generates the *a posteriori* symbol probability for each bit  $x_n^i$ ,

$$\Lambda_i[n] \triangleq \log \frac{P(x_n^i = 1 | \mathbf{Y})}{P(x_n^i = 0 | \mathbf{Y})}, \quad (1)$$

where  $\mathbf{Y}$  denotes the received signal which is given by (3). Based on this posterior information, the soft MDSQ decoding rule is given by

$$\begin{aligned} (\hat{I}_1(j), \hat{I}_2(j)) &= \arg \max_{(l,m) \in \mathcal{C}} P(I_1(j) = l | \{\Lambda_1[n]\}_n) \\ &\cdot P(I_2(j) = m | \{\Lambda_2[n]\}_n), \end{aligned} \quad (2)$$

which maximizes the posterior probability of the indices subject to a code structure constraint, that is,  $(I_1(j), I_2(j)) \in \mathcal{C}$ .

## 2.2. Signal model for diversity OFDM system

Consider an OFDM system with  $N$ -subcarriers signaling through a frequency-selective fading channel. The channel response is assumed to be constant during one symbol duration. The block diagram of such a system is shown in Figure 4. The diversity OFDM system is just the parallel concatenation of combination of two such OFDM systems.

The binary information data  $\{a_n^i\}_n$  are grouped and mapped into multiphase signals, which take values from a finite alphabet set  $\mathcal{A} = \{\beta_1, \dots, \beta_{|\mathcal{A}|}\}$ . In this paper, QPSK modulation is employed. The QPSK signals  $\{d_k^i\}_{k=0}^{N-2}$  are differentially encoded to resolve the phase ambiguity inherent in any blind receiver, and the output is given by  $Z_k^i = Z_{k-1}^i d_k^i$ . These differentially encoded symbols are then inverse DFT transformed. A guard interval is inserted to prevent possible interference between OFDM frames. After pulse shaping and parallel-to-serial conversion, the signals are transmitted through a frequency-selective fading

channel. At the receiver end, after matched-filtering and removing the guard interval, the sampled received signals are sent to a DFT block to demultiplex the multicarrier signals.

For the  $i$ th OFDM system with proper cyclic extensions and proper sample timing, the demultiplexing sample of the  $k$ th subcarrier can be expressed as [10]

$$Y_k^i = Z_k^i H_k^i + V_k^i, \quad k = 0, 1, \dots, N-1; i = 1, 2, \quad (3)$$

where  $V_k^i \sim \mathcal{N}_c(0, \sigma^2)$  is the i.i.d. complex Gaussian noise and  $H_k^i$  is the channel frequency response at the  $k$ th subcarrier. Using the fact that  $H_k^i$  can be further expressed as a DFT transformation of the channel time response, the signal model (3) becomes

$$Y_k^i = Z_k^i \mathbf{w}_f^H(k) \mathbf{h}^i + V_k^i, \quad k = 0, 1, \dots, N-1; i = 1, 2, \quad (4)$$

where  $\mathbf{h}^i = [h_0^i, h_1^i, \dots, h_{L-1}^i]^T$  contains the time responses of all  $L$  taps;  $L \triangleq \lceil \tau_m \Delta_f + 1 \rceil$  denotes the maximum number of resolvable taps, with  $\tau_m$  being the maximum multipath spread and  $\Delta_f$  being the tone spacing of the carriers; and  $\mathbf{w}_f(k) \triangleq [1, e^{-j2\pi k/N}, \dots, e^{-j2\pi k(L-1)/N}]^T$  contains the corresponding DFT coefficients.

## 3. TURBO RECEIVER

The receiver under consideration is an iterative receiver structure as shown in Figure 5. It consists of two blind Bayesian OFDM detectors, which compute the soft information for the corresponding descriptions. At the output of the blind detector, information about one description is transferred to the other based on the existence of correlation between the two descriptions. Such information transfer is then repeated between the two blind detectors to improve the system performance. Next, we will focus on the operation on the first description to illustrate the iterative procedure.

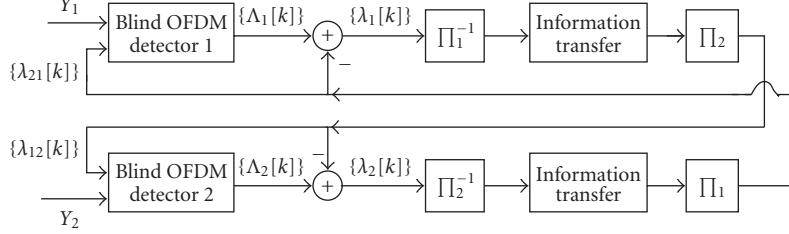


FIGURE 5: Turbo decoding for multiple description over a diversity OFDM system;  $\Pi_i$  and  $\Pi_i^{-1}$  denote the interleaver and deinterleaver, respectively, for the  $i$ th description.

### 3.1. Blind Bayesian OFDM detector

Denote  $\mathbf{Y}^1 \triangleq \{Y_0^1, Y_1^1, \dots, Y_{N-1}^1\}$  as the received signals for the first description. The blind Bayesian OFDM detector for the first description computes the *a posteriori* probabilities of the information bits  $\{a_n^1\}_n$ ,

$$\Lambda_1[n] \triangleq \log \frac{P(a_n^1 = 1 | \mathbf{Y}^1)}{P(a_n^1 = 0 | \mathbf{Y}^1)}. \quad (5)$$

The design of such a blind Bayesian detector will be discussed later in Section 4. For now, we assume the Bayesian detector provides us such soft information, and focus on the structure of the turbo receiver.

The *a posteriori* information delivered by the blind detector can be further expressed as

$$\Lambda_1[n] = \underbrace{\log \frac{P[\mathbf{Y}^1 | a_n^1 = 1]}{P[\mathbf{Y}^1 | a_n^1 = 0]}}_{\lambda_1[n]} + \underbrace{\log \frac{P[a_n^1 = 1]}{P[a_n^1 = 0]}}_{\lambda_{21}^p[n]}. \quad (6)$$

The second term in (6), denoted by  $\lambda_{21}^p[n]$ , represents the *a priori* log-likelihood ratio (LLR) of the bit  $a_n^1$  fed from detector 2. The superscript  $p$  indicates the quantity obtained from the previous iteration. The first term in (6), denoted by  $\lambda_1[n]$ , represents the *extrinsic* information delivered by detector 1, based on the received signals  $\mathbf{Y}^1$ , the structure of signal model (4), and the *a priori* information about all other bits  $\{a_l^1\}_{l \neq n}$ . The extrinsic information  $\{\lambda_1[n]\}$  is transformed into *a priori* information  $\{\lambda_{12}^p[n]\}$  for bits  $\{a_n^2\}_n$ . This information transformation procedure is described next.

### 3.2. Information transformation

Assume that  $\{a_n^i\}_n$  is mapped to  $\{x_n^i\}_n$  after passing through the  $i$ th deinterleaver  $\Pi_i^{-1}$ , with  $x_n^i \triangleq a_{\pi_i(n)}^i$ . To transfer the information from detector 1 to detector 2, the following steps are required.

- (1) Compute the bit probability of the deinterleaved bits

$$P(x_n^1 = 1) = \frac{e^{\lambda_1[\pi_1(n)]}}{1 + e^{\lambda_1[\pi_1(n)]}}. \quad (7)$$

- (2) Compute the probability distribution for the first index  $I_1$  based on the deinterleaved bit probabilities

$$P(I_1(j) = l) = \prod_{k=1}^R P(x_{(j-1)R+k}^1 = b_k(l)), \quad l = 1, \dots, |\mathcal{J}|, \quad (8)$$

where  $\{b_k(l), k = 1, \dots, R\}$  is the binary representation for the index  $l \in \mathcal{J}$ . Recall that  $R$  denotes the bit length of each description.

- (3) Compute the probability distribution for the second index  $I_2$  according to

$$P(I_2(j) = m) = \sum_{l=1}^{|\mathcal{J}|} P(I_2(j) = m | I_1(j) = l) \cdot P(I_1(j) = l), \quad m = 1, \dots, |\mathcal{J}|. \quad (9)$$

- (4) Compute the bit probability that is associated with index  $I_2(j)$ ,

$$P(x_{(j-1)R+k}^2 = 1) = \sum_{m: b_l(m)=1} P(I_2(j) = m). \quad (10)$$

- (5) Compute the log likelihood of interleaved code bit

$$\lambda_{12}[\pi_2(n)] = \log \frac{P(x_n^2 = 1)}{1 - P(x_n^2 = 1)}. \quad (11)$$

It is important to mention here that the key step is the calculation of the conditional probability  $P(I_2(j) = m | I_1(j) = l)$  in (9). Hence, the proposed turbo receiver exploits the correlation between the two descriptions, which is measured by the conditional probabilities in (9). From the discussion in

the previous section, these conditional probabilities can be easily obtained from the index assignment rule  $\alpha(\cdot)$  as shown in Figure 3.

#### 4. BLIND BAYESIAN OFDM DETECTOR

##### 4.1. Problem statement

Denote  $\mathbf{Y}^i \triangleq \{Y_0^i, Y_1^i, \dots, Y_{N-1}^i\}$ . The Bayesian OFDM receiver estimates the *a posteriori* probabilities of the information symbols

$$P(d_k^i = \beta_l \mid \mathbf{Y}^i), \quad \beta_l \in \mathcal{A}; k = 1, \dots, N-1, \quad (12)$$

based on the received signals  $\mathbf{Y}^i$  and the *a priori* symbol probabilities of  $\{d_k^i\}_{k=1}^{N-1}$ , without knowing the channel response  $\mathbf{h}^i$ . Assume the bit  $a_n^i$  is mapped to symbol  $d_{\kappa(n)}^i$ . Based on this symbol *a posteriori* probability, the LLR of the code bit as required in (5) can be computed by

$$\begin{aligned} \Lambda_i[n] &\triangleq \log \frac{P(a_n^i = 1 \mid \mathbf{Y}^i)}{P(a_n^i = 0 \mid \mathbf{Y}^i)} \\ &= \log \frac{\sum_{\beta_l \in \mathcal{A}: d_{\kappa(n)}^i = \beta_l, a_n^i = 1} P(d_{\kappa(n)}^i = \beta_l \mid \mathbf{Y}^i)}{\sum_{\beta_l \in \mathcal{A}: d_{\kappa(n)}^i = \beta_l, a_n^i = 0} P(d_{\kappa(n)}^i = \beta_l \mid \mathbf{Y}^i)}. \end{aligned} \quad (13)$$

Assume that the unknown quantities  $\mathbf{h}^i$ ,  $\mathbf{Z}^i \triangleq \{Z_k^i\}_{k=1}^{N-1}$  are independent of each other and have *a priori* distribution  $p(\mathbf{h}^i)$  and  $p(\mathbf{Z}^i)$ , respectively. The direct computation of (12) is given by

$$P(d_k^i = a_l \mid \mathbf{Y}^i) \propto \sum_{\mathbf{Z}^i: d_k^i = a_l} \int p(\mathbf{Y}^i \mid \mathbf{h}^i, \mathbf{Z}^i) p(\mathbf{h}^i) p(\mathbf{Z}^i) d\mathbf{h}^i, \quad (14)$$

where  $p(\mathbf{Y}^i \mid \mathbf{h}^i, \mathbf{Z}^i)$  is a Gaussian density function [cf. (4)]. Clearly, the computation in (14) involves a very high-dimensional integration which is certainly infeasible in practice. Therefore, we resort to the sequential Monte Carlo method for numerical evaluation of the above multidimensional integration.

##### 4.2. SMC-based blind MAP detector

Sequential Monte Carlo (SMC) is a family of methodologies that use Monte Carlo simulations to efficiently estimate the *a posteriori* distributions of the unknown states in a dynamic system [11, 12, 13]. In [14], an SMC-based blind MAP symbol detection algorithm for OFDM systems is proposed. This algorithm is summarized as follows.

- (0) Initialization. Draw the initial samples of the channel vector from  $\mathbf{h}_{-1}^{(j)} \sim N_c(\mathbf{0}, \Sigma_{-1})$ , for  $j = 1, \dots, m$ . All importance weights are initialized as  $w_{-1}^{(j)} = 1$ ,  $j = 1, \dots, m$ .

The following steps are implemented at the  $k$ th recursion ( $k = 0, \dots, N-1$ ) to update each weighted sample. For  $j = 1, \dots, m$ , the following hold.

- (1) For each  $a_i \in \mathcal{A}$ , compute the following quantities:

$$\begin{aligned} \mu_{k,i}^{(j)} &= a_i \mathbf{w}_f^H(k) \mathbf{h}_{k-1}^{(j)}, \\ \sigma_{k,i}^{2(j)} &= \sigma^2 + \mathbf{w}_f^H(k) \Sigma_{k-1}^{(j)} \mathbf{w}_f(k), \\ \alpha_{k,i}^{(j)} &= \frac{1}{\pi \sigma_{k,i}^{2(j)}} \exp \left\{ -\frac{\|Y_k - \mu_{k,i}^{(j)}\|^2}{\sigma_{k,i}^{2(j)}} \right\} \cdot P(d_k = a_i Z_{k-1}^{(j)*}). \end{aligned} \quad (15)$$

- (2) Impute the symbol  $Z_k$ . Draw  $Z_k^{(j)}$  from the set  $\mathcal{A}$  with probability

$$P(Z_k = a_i \mid \mathbf{Z}_{k-1}^{(j)}, \mathbf{Y}_k) \propto \alpha_{k,i}^{(j)}, \quad a_i \in \mathcal{A}. \quad (16)$$

- (3) Compute the importance weight:

$$w_k^{(j)} = w_{k-1}^{(j)} \cdot \sum_{a_i \in \mathcal{A}} \alpha_{k,i}^{(j)}. \quad (17)$$

- (4) Update the *a posteriori* mean and covariance of the channel. If the imputed sample  $Z_k^{(j)} = a_i$  in step (2), set  $\mu_k^{(j)} = \mu_{k,i}^{(j)}$ ,  $\sigma_k^{2(j)} = \sigma_{k,i}^{2(j)}$ ; and update

$$\begin{aligned} \mathbf{h}_k^{(j)} &= \mathbf{h}_{k-1}^{(j)} + \frac{Y_k - \mu_k^{(j)}}{\sigma_k^{2(j)}} \boldsymbol{\xi}, \\ \Sigma_k^{(j)} &= \Sigma_{k-1}^{(j)} - \frac{1}{\sigma_k^{2(j)}} \boldsymbol{\xi} \boldsymbol{\xi}^T, \end{aligned} \quad (18)$$

with

$$\boldsymbol{\xi} \triangleq \Sigma_{k-1}^{(j)} \mathbf{w}_f(k) Z_k^{(j)*}. \quad (19)$$

- (5) Perform resampling when  $k$  is a multiple of  $k_0$ , where  $k_0$  is the resampling interval.

##### 4.3. APP detection

The above sampling procedure generates a set of random samples  $\{(\mathbf{Z}_k^{(j)}, w_k^{(j)})\}_{j=1}^m$ , properly weighted with respect to the distribution  $p(\mathbf{Z}_k \mid \mathbf{Y}_k)$ . Based on these samples, an online estimation and a delayed-weight estimation can be obtained straightforwardly as

$$\begin{aligned} P(d_k = \beta_l \mid \mathbf{Y}_k) &\cong \frac{1}{W_k} \sum_{j=1}^m \mathbb{1}(Z_{k+1}^{(j)} Z_k^{(j)*} = \beta_l) w_k^{(j)}, \\ P(d_k = \beta_l \mid \mathbf{Y}_{k+\delta}) &\cong \frac{1}{W_{k+\delta}} \sum_{j=1}^m \mathbb{1}(Z_{k+1}^{(j)} Z_k^{(j)*} = \beta_l) w_{k+\delta}^{(j)}, \end{aligned} \quad (20)$$

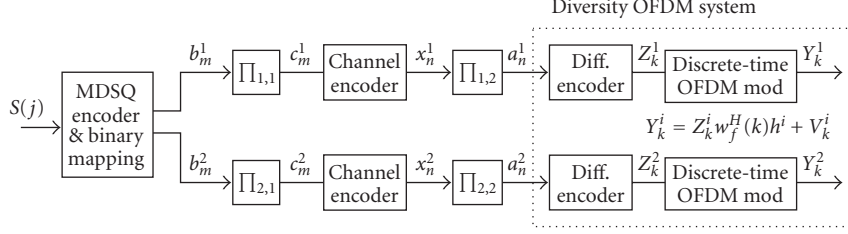


FIGURE 6: MDSQ over a channel-coded diversity OFDM system.

where  $W_k \triangleq \sum_j w_k^{(j)}$ , and  $\mathbf{1}(\cdot)$  denotes the indicator function. Note that both of these two estimates are only approximations to the *a posteriori* symbol probability  $P(d_k = \beta_l | \mathbf{Y}_{N-1})$ .

We next propose a novel APP estimator, where the channel is estimated as a mixture vector, based on which the symbol APPs are then computed. Specifically, we have

$$p(\mathbf{h} | \mathbf{Y}_{N-1}) = \frac{1}{W_{N-1}} \sum_{j=1}^m \underbrace{p(\mathbf{h} | \mathbf{Y}_{N-1}, \mathbf{Z}_{N-1}^{(j)})}_{\mathcal{N}_c(\mathbf{h}_{N-1}^{(j)}, \Sigma_{N-1}^{(j)})} \cdot w_{N-1}^{(j)}. \quad (21)$$

The symbol *a posteriori* probability is then given by

$$\begin{aligned} P(d_k = \beta_l | \mathbf{Y}_{N-1}) &= \int P(d_k = \beta_l | \mathbf{Y}_{N-1}, \mathbf{h}) p(\mathbf{h} | \mathbf{Y}_{N-1}) d\mathbf{h} \\ &= \int P(d_k = \beta_l | \mathbf{Y}_{N-1}, \mathbf{h}) \\ &\quad \times \left[ \frac{1}{W_{N-1}} \sum_{j=1}^m p(\mathbf{h} | \mathbf{Y}_{N-1}, \mathbf{Z}_{N-1}^{(j)}) \cdot w_{N-1}^{(j)} \right] d\mathbf{h} \\ &= \frac{1}{W_{N-1}} \sum_{j=1}^m w_{N-1}^{(j)} \cdot \left[ \int P(d_k = \beta_l | \mathbf{Y}_{N-1}, \mathbf{h}) \right. \\ &\quad \cdot p(\mathbf{h} | \mathbf{Y}_{N-1}, \mathbf{Z}_{N-1}^{(j)}) d\mathbf{h} \Bigg] \\ &\approx \frac{1}{W_{N-1}} \sum_{j=1}^m w_{N-1}^{(j)} \\ &\quad \cdot \left[ P(d_k = \beta_l) \sum_{Z_k Z_{k-1}^* = \beta_l} \int P(\mathbf{Y}_{k-1}^k | \mathbf{Z}_{k-1}^k, \mathbf{h}) \right. \\ &\quad \cdot p(\mathbf{h} | \mathbf{Y}_{N-1}, \mathbf{Z}_{N-1}^{(j)}) d\mathbf{h} \Bigg], \end{aligned} \quad (22)$$

where  $\mathbf{Y}_{k-1}^k \triangleq [Y_{k-1}, Y_k]^T$ ,  $\mathbf{Z}_{k-1}^k \triangleq [Z_{k-1}, Z_k]^T$ . Note that the integral within (22) is an integral of a Gaussian pdf with respect to another Gaussian pdf. The resulting distribution is

still Gaussian, that is,

$$\begin{aligned} &\int P(\mathbf{Y}_{k-1}^k | \mathbf{Z}_{k-1}^k, \mathbf{h}) \cdot p(\mathbf{h} | \mathbf{Y}_{N-1}, \mathbf{Z}_{N-1}^{(j)}) d\mathbf{h} \\ &\sim \mathcal{N}_c(\boldsymbol{\mu}_{k,j}(\mathbf{Z}_{k-1}^k), \boldsymbol{\Sigma}_{k,j}(\mathbf{Z}_{k-1}^k)), \end{aligned} \quad (23)$$

with mean and variance given, respectively, by

$$\begin{aligned} \boldsymbol{\mu}_{k,j}(\mathbf{Z}_{k-1}^k) &= \begin{bmatrix} \mu_{k,j}(Z_k) \\ \mu_{k-1,j}(Z_{k-1}) \end{bmatrix}, \quad \text{with } \mu_{k,j}(x) \triangleq x \mathbf{w}_k^H \mathbf{h}_{N-1}^{(j)}, \\ \boldsymbol{\Sigma}_{k,j}(\mathbf{Z}_{k-1}^k) &= \begin{bmatrix} \sigma_{k,j}^2 & 0 \\ 0 & \sigma_{k-1,j}^2 \end{bmatrix}, \quad \text{with } \sigma_{k,j}^2 \triangleq \mathbf{w}_k^H \boldsymbol{\Sigma}_{N-1}^{(j)} \mathbf{w}_k + \sigma^2. \end{aligned} \quad (24) \quad (25)$$

Equations (24) and (25) follow from the fact that conditioned on the channel  $\mathbf{h}$ ,  $Y_k$  and  $Y_{k+1}$  are independent. The symbol *a posteriori* probability can then be computed in a close form as

$$\begin{aligned} &P(d_k = \beta_l | \mathbf{Y}_{N-1}) \\ &\approx \sum_{j=1}^m \sum_{Z_k Z_{k-1}^* = \beta_l} w_N^{(j)} \\ &\quad \cdot \frac{P(d_k = \beta_l)}{\sigma_{k,j}^2 + \sigma_{k-1,j}^2} \exp \left\{ - \frac{|Y_k - \mu_{k,j}(Z_k)|^2}{\sigma_{k,j}^2} \right. \\ &\quad \left. - \frac{|Y_{k-1} - \mu_{k-1,j}(Z_{k-1})|^2}{\sigma_{k-1,j}^2} \right\}. \end{aligned} \quad (26)$$

## 5. CHANNEL-CODED SYSTEMS

Although the MDSQ introduces some redundancy to the system, it has limited capability for error correction. In order to improve the system reliability, we next consider introducing channel coding to the proposed MDSQ system.

A block diagram of an MDSQ system over a channel-coded diversity OFDM system is shown in Figure 6. A stream of source signal  $\{S(j)\}_j$  is MDSQ encoded, resulting in two sets of indices  $\{I_1(j), I_2(j)\}_j$ . Binary descriptions of these

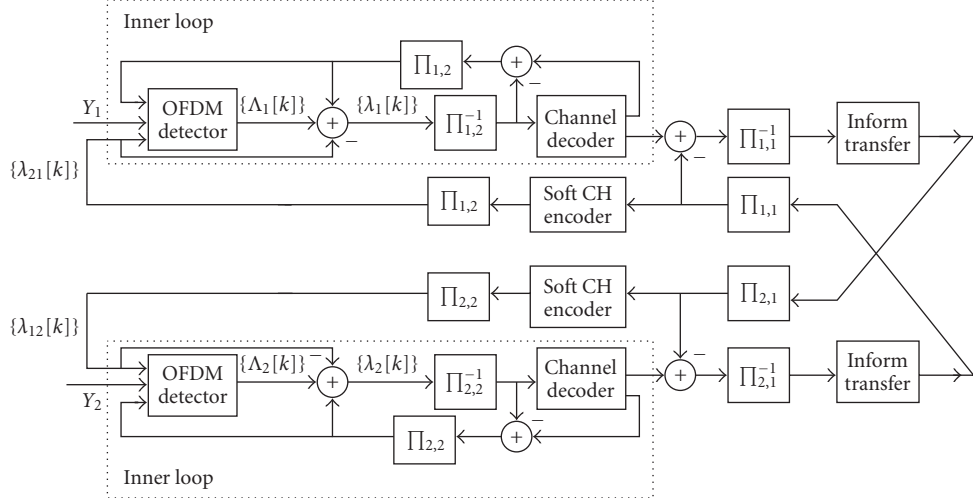


FIGURE 7: Turbo decoding for MDSQ over a channel-coded diversity OFDM system.

indices,  $\{b_m^1, b_m^2\}_m$ , are then channel encoded and OFDM modulated. There are two sets of bit interleavers in the system: one set, named  $\{\Pi_{i,1}\}_{i=1}^2$ , is applied between the MDSQ encoder and channel encoder; the other set, named  $\{\Pi_{i,2}\}_{i=1}^2$ , is applied between the channel encoder and OFDM modulator.

At the receiver, a novel blind iterative receiver is developed for joint demodulation, channel decoding, and MDSQ decoding. The receiver structure, as shown in Figure 7, consists of two loops of iterative operations. For each description, there is an inner loop (iterative procedure) for joint OFDM demodulation and channel decoding. At the outer loop, soft information of the coded bits is exchanged between the two inner loops to exploit the correlations between the two descriptions. Next, we discuss the operation of both the inner loop and the outer loop.

#### *Inner loop: joint OFDM demodulation and channel decoding*

We consider a subsystem of the original MDSQ system, which consists of the channel coding and OFDM modulation for only one source description. Since the combination of a differential encoder and OFDM system acts as an inner encoder, the above subsystem is a typical serial concatenated code, and an iterative (turbo) receiver can be designed for such a system, which is denoted as the inner loop part in Figure 7. It consists of two stages: the SMC OFDM detector developed in the previous sections, followed by a MAP channel decoder [15]. The two stages are separated by a deinterleaver and an interleaver. Note that both the SMC OFDM detector and the MAP channel decoder can incorporate the *a priori* probabilities and output *a posteriori* probabilities of the code bits  $\{a_n^i\}_n$ , that is, they are soft-input and soft-output algorithms. Based on the turbo principle, extrinsic information of the channel-coded bits can be

exchanged iteratively between the SMC OFDM detector and the MAP channel decoder to improve the performance of the subsystem.

#### *Outer loop: exploiting the correlation between the two descriptions*

In Section 3, an iterative receiver was proposed for joint MDSQ decoding and OFDM demodulation. Extrinsic information from one description is transformed into the soft information for the other description, and is fed into the OFDM demodulator as the *a priori* information. For channel-coded MDSQ systems, similar approaches can be considered to exploit the correlation between the two descriptions. As shown in Figure 7, the MAP channel decoder incorporates the *a priori* information for the channel-coded bits, and outputs the *a posteriori* probability of both channel-coded bits and uncoded bits. On the other hand, the OFDM detector incorporates and produces as output only the soft information for the channel-coded bits. Taking into account that only uncoded bits will be considered in the MDSQ decoder, the inner loop, when considered as one unit operation, is a SISO algorithm that incorporates the *a priori* information of the channel-coded bits, and produces the output *a posteriori* information of the uncoded bits. Altogether, the two inner loops constitute a turbo structure in parallel, and the transferred soft information provided by the information transformation block (IF-T) can be exchanged iteratively between the two inner loops. This iterative procedure is the outer loop of the system, which aims at further improving the system performance by exploiting the correlation between the two descriptions. It is shown in Section 3 that this correlation can be measured by the probability transformation matrix, and adopted by the IF-T block. For the outer loop, the soft output of the inner loop can be used directly as the *a priori* information for

the IF-T; the soft output of IF-T, however, must be transformed before being fed into the inner loop as *a priori* information. Specifically, a soft channel encoder by the BCJR algorithm [15] is required to transform the soft information of the uncoded bits into the soft information of the coded bits.

## 6. SIMULATION RESULTS

In this section, we provide computer simulation results to illustrate the performance of the turbo receiver for MDSQ over diversity OFDM systems. In the simulations, the continuous alphabet source is assumed to be uniformly distributed on  $(-1, 1)$ , and a uniform quantizer is applied. The source range is divided into 8, 22, and 34 intervals. Two indices are assigned to describe the source according the index assignment  $\alpha(\cdot)$  as shown in Figure 3, where each index is described with  $R = 3$  bits. Assume the channel bandwidth for each OFDM system is divided into  $N = 128$  subchannels. Guard interval is long enough to protect the OFDM blocks from intersymbol interference due to the delay spread. The frequency-selective fading channels are assumed to be uncorrelated. All  $L = 5$  taps of the fading channel are Rayleigh distributed with the same variance, normalized such that  $E\{\sum_{n=0}^{L-1} \|h_n\|^2\} = 1$ , and have delays  $\tau_l = l/\Delta_f$ ,  $l = 0, 1, \dots, L - 1$ . For channel-coded systems, a rate-1/2 constraint length-5 convolutional code (with generators 23 and 35 in octal notation) is used. The interleavers are generated randomly and fixed for all simulations.

The blind SMC detector implements the algorithm described in Section 4.2. The variance of the noise  $V_k$  in (24) is assumed known at the detector with values specified by the given SNR. The SMC algorithm draws  $m = 50$  Monte Carlo samples at every recursion with  $\Sigma_{-1}$  set to  $1000\mathbf{I}_L$ . Two qualities were used in the simulation to measure the performance of the SMC detector: bit error rate (BER) and word error rate (WER). Here, the bit error rate denotes the information bit error rate and word error rate denotes the error rate of the whole data block transferred during one symbol duration. On the other hand, mean square error (MSE) will be used to measure the performance of the whole system.

### Performance of the SMC detector

The blind SMC detector, as a SISO algorithm for OFDM demodulation, is an important component of the proposed turbo receiver. Next, we illustrate the performance of the blind SMC detector. In Figure 8, the BER and WER performance is plotted. In the same figure, we also plot the known channel lower bound, where the fading coefficients are assumed to be perfectly known to the receiver and a MAP receiver is employed to compute the *a posteriori* symbol probabilities.

Although the SMC detector generates soft outputs in terms of the symbol *a posteriori* probabilities, only hard decisions are used in an uncoded system. However in a coded system, the channel decoder, such as a MAP decoder, requires

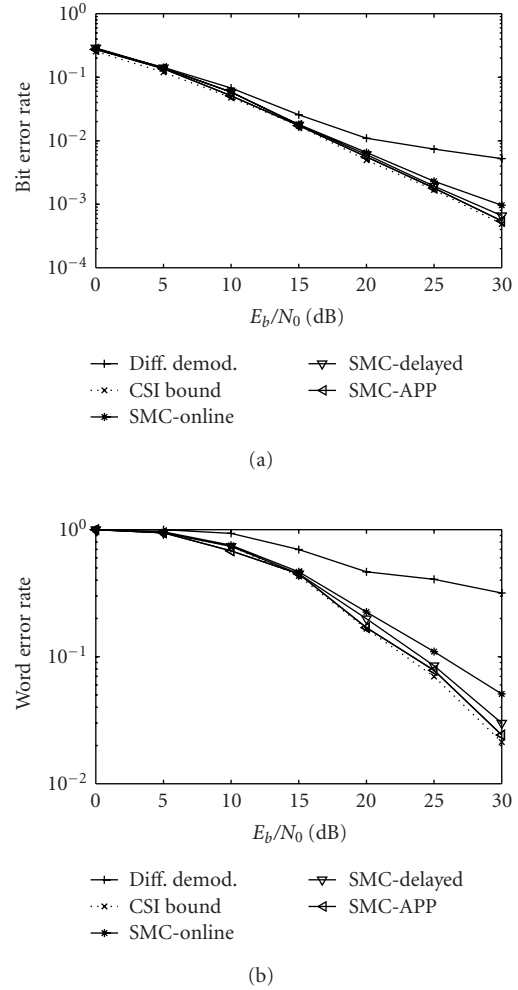


FIGURE 8: The (a) BER and (b) WER performance in an uncoded OFDM system.

soft information provided by the demodulator. Next, we examine the accurateness of the soft output provided by the SMC detector in a coded OFDM scenario. In Figure 9, the BER and WER performance for the information bits is plotted. In the same figure, the known channel lower bound is also plotted. The MAP convolutional decoder is employed in conjunction with the different detection algorithms. It is seen from Figure 9 that the three SMC detector yield different performance after the MAP decoder because of the different quality of the soft information they provide. Specifically, the APP detector achieves the best performance.

### Performance of turbo receiver for MDSQ system

The performance of the turbo receiver is shown in Figures 10, 11, and 12 for MDSQ systems with assignments 8, 22, and 34, respectively, as in Figure 3. The SMC blind detector is employed. In each figure, the BER, WER, and MSE are plotted. In the same figure, the quantization error bound  $s^2/12$ , where

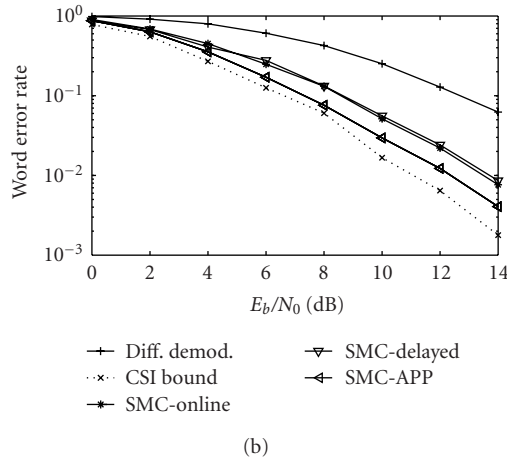
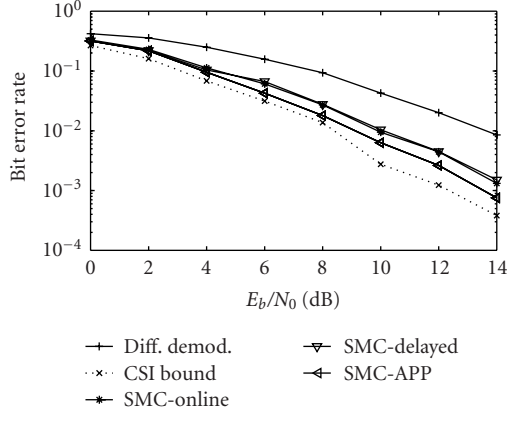


FIGURE 9: The (a) BER and (b) WER performance in a channel-coded OFDM system.

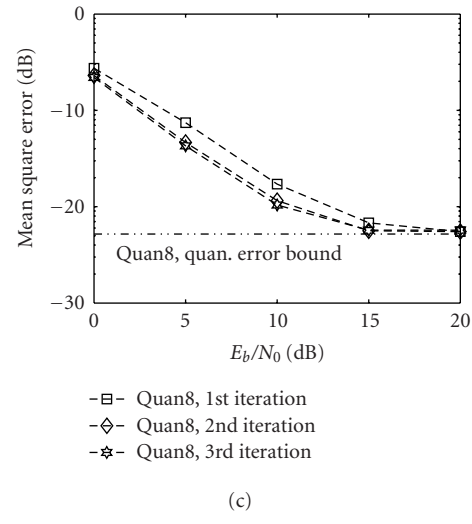
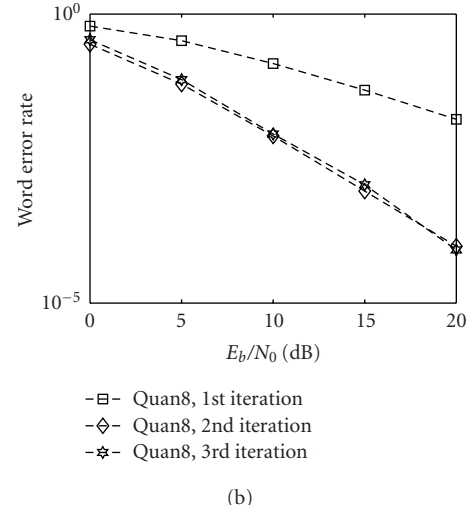
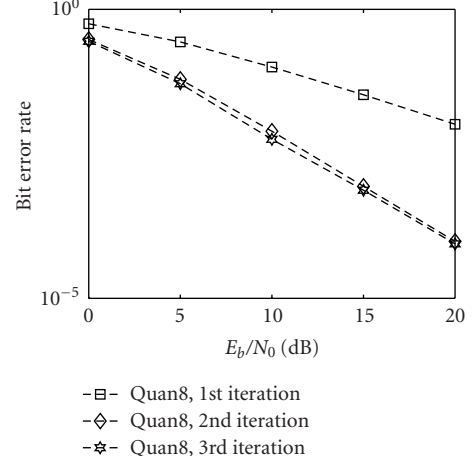


FIGURE 10: Performance of iterative receiver for the MDSQ system with  $N = 8$ . (a) BER. (b) WER. (c) MSE.

$s$  denote the quantization interval, is also plotted in a dotted line. It is seen that the BER and WER performance is significantly improved at the second iteration, that is, 15 dB better for  $N = 8$ , 4 dB better for  $N = 22$  and 2 dB better for  $N = 34$ . However, no significant gain is achieved by more iterations. Note that the MSEs of the turbo receivers are very close to the quantization error bound at high SNR. The quantization error bound ( $5.2 \times 10^{-3}$ ) for  $N = 8$  is achieved at about 15 dB. However, much lower quantization error bounds are achieved at higher SNR by the turbo receiver with  $N = 22$  and 34, that is,  $6.9 \times 10^{-4}$  for  $N = 22$  at SNR = 25 dB and  $2.8 \times 10^{-4}$  for  $N = 34$  at SNR = 30 dB. Moreover, due to the different quantization error bounds determined by  $N$  and the BER and the WER performance achieved by the turbo receiver, different MDSQ scheme should be chosen at different SNRs to minimize the MSE. For example, the MDSQ with  $N = 8$  is superior to other assignments below SNR = 10 dB. However, at SNR = 20 dB, the MDSQ scheme with  $N = 22$  is the best choice among the three assignments considered in this paper.

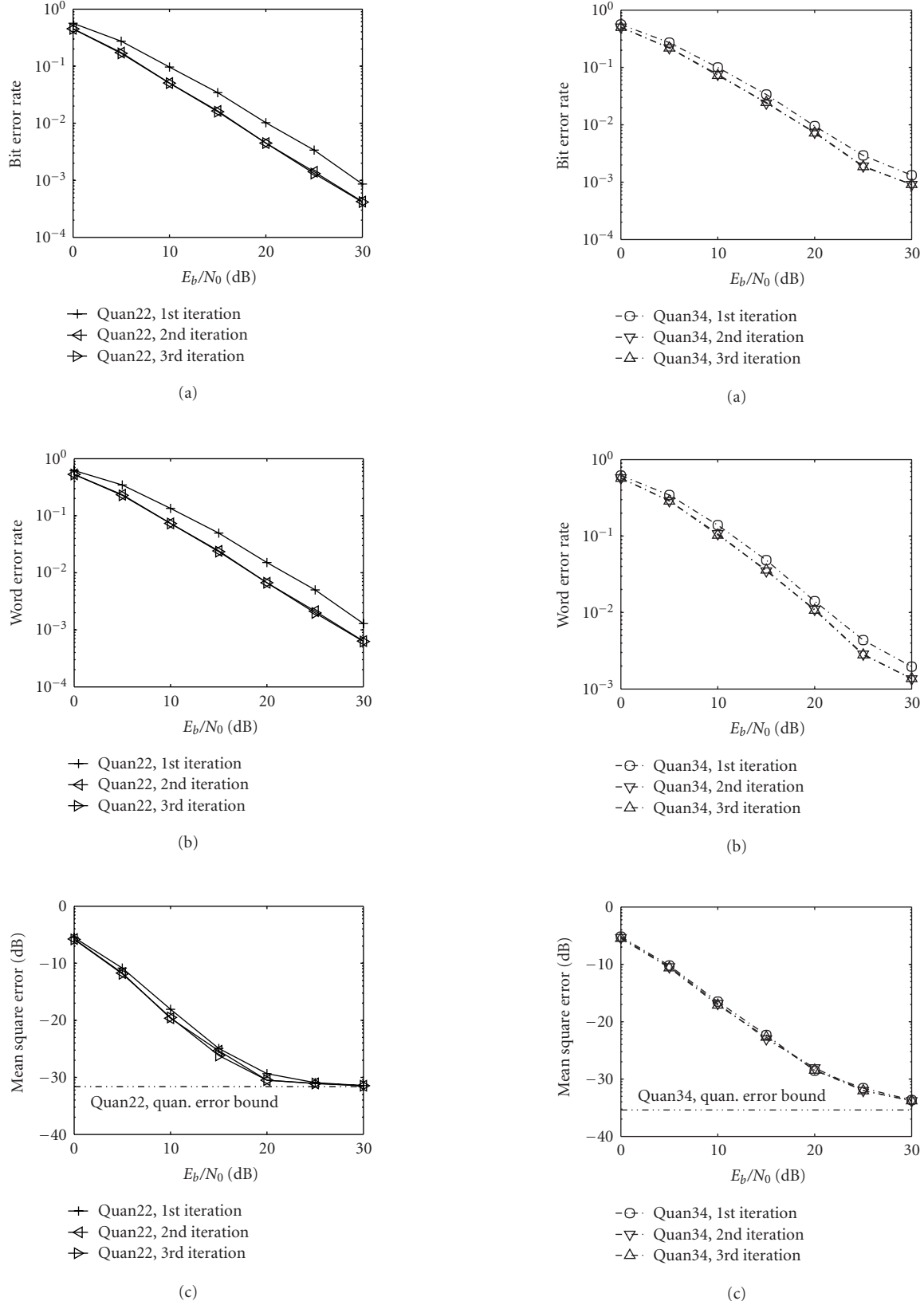


FIGURE 11: Performance of iterative receiver for the MDSQ system with  $N = 22$ . (a) BER. (b) WER. (c) MSE.

FIGURE 12: Performance of iterative receiver for the MDSQ system with  $N = 34$ . (a) BER. (b) WER. (c) MSE.

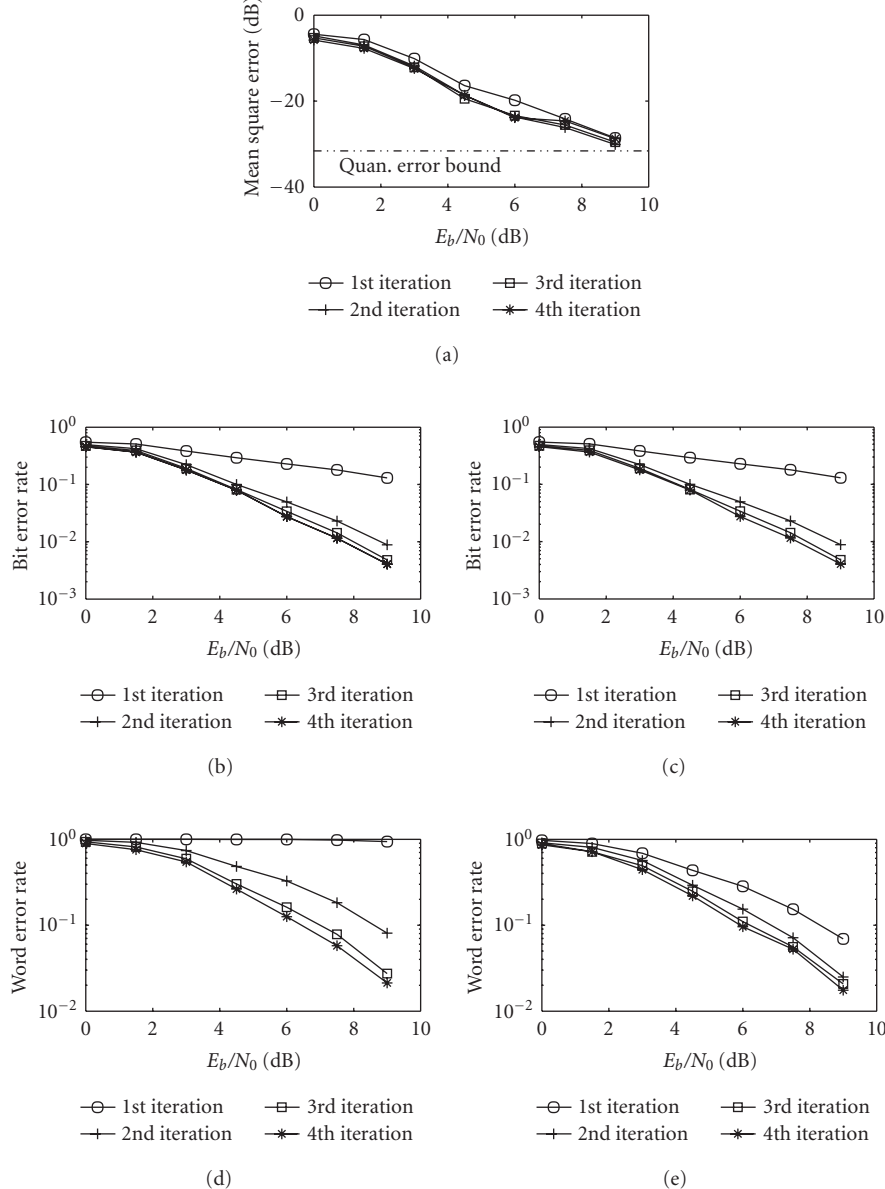


FIGURE 13: Performance of iterative receiver for channel coded MDSQ system, with 1 iteration for inner loop and 4 iterations for outer loop.  
(a) MSE. (b) BER of coded bits. (c) BER of information bits. (d) WER of coded bits. (e) WER of information bits.

#### Performance of turbo receiver for channel-coded MDSQ system

Finally, we consider the performance of the channel-coded MDSQ system discussed in Section 5. Performance is compared for systems with different iterative profiles. Specifically, the BER, WER, and MSE performance for the information bits and coded bits are plotted in Figures 13 and 14 for the 4-inner-loop and 1-outer-loop turbo receivers and the 3-inner-loop and 2-outer-loop turbo receivers, respectively. In the simulation, the source range is divided into 22 intervals as shown in Figure 3b. It is seen that the proposed turbo receiver structure can successively improve

the receiver performance through iterative processing. Moreover, the quantization error bounds are achieved at very low SNR, that is, 10 dB.

## 7. CONCLUSIONS

In this paper, we have proposed a blind turbo receiver for transmitting MDSQ-coded sources over frequency-selective fading channels. Transformation of the extrinsic information of the two descriptions are exchanged between each other to improve the system performance. A novel blind APP OFDM detector, which computes the *a posteriori* symbol

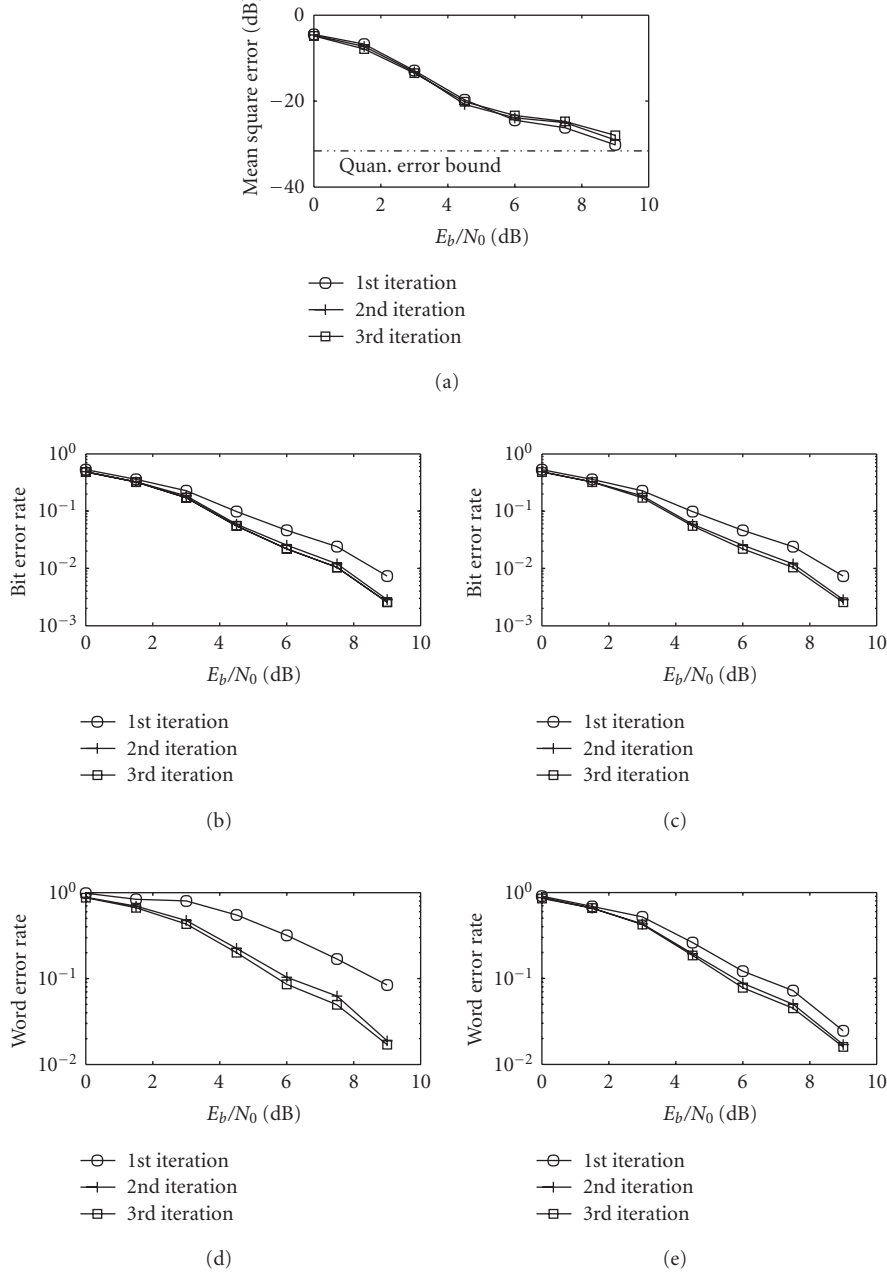


FIGURE 14: Performance of iterative receiver for channel-coded MDSQ system, with 2 iterations for inner loop and 3 iterations for outer loop. (a) MSE. (b) BER of coded bits. (c) BER of information bits. (d) WER of coded bits. (e) WER of information bits.

probabilities, is developed using sequential Monte Carlo (SMC) techniques. Being soft-input and soft-output in nature, the proposed SMC detector is capable of exchanging the so-called extrinsic information with other component in the above turbo receiver, and successively improving the overall receiver performance. Finally, we have also treated channel-coded systems, and a novel blind turbo receiver is developed for joint demodulation, channel decoding, and MDSQ decoding. Simulation results have demonstrated the effectiveness of the proposed techniques.

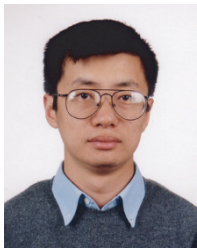
## REFERENCES

- [1] A. E. Gamal and T. Cover, “Achievable rates for multiple descriptions,” *IEEE Trans. Inform. Theory*, vol. 28, no. 6, pp. 851–857, 1982.
- [2] V. Vaishampayan, “Design of multiple description scalar quantizers,” *IEEE Trans. Inform. Theory*, vol. 39, no. 3, pp. 821–834, 1993.
- [3] Y. Zhang, M. Motani, and H. Garg, “Wireless video transmission using multiple description codes combined with prioritized DCT compression,” in *IEEE International Conference on*

- Multimedia and Expo (ICME '02)*, vol. 1, pp. 261–264, Lausanne, Switzerland, August 2002.
- [4] L. Ozarow, “On a source coding problem with two transmitters and three receivers,” *Bell Labs Technical Journal*, vol. 59, no. 10, pp. 1909–1921, 1980.
  - [5] S.-M. Yang and V. Vaishampayan, “Low-delay communication for Rayleigh fading channels: an application of the multiple description quantizer,” *IEEE Trans. Commun.*, vol. 43, no. 11, pp. 2771–2783, 1995.
  - [6] J. Barros, J. Hagenauer, and N. Gortz, “Turbo cross decoding of multiple descriptions,” in *Proc. IEEE International Conference on Communications (ICC '02)*, vol. 3, pp. 1398–1402, New York, NY, USA, April 2002.
  - [7] N. Kamaci, Y. Altunbasak, and R. Mersereau, “Multiple description coding with multiple transmit and receive antennas for wireless channels: the case of digital modulation,” in *IEEE Global Telecommunications Conference (GLOBECOM '01)*, pp. 3272–3276, San Antonio, Tex, USA, November 2001.
  - [8] D. Sachs, R. Anand, and K. Ramchandran, “Wireless image transmission using multiple-description based concatenated codes,” in *Proc. IEEE Data Compression Conference (DCC '00)*, p. 569, Snowbird, Utah, USA, March 2000.
  - [9] K. Balachandran and J. Anderson, “Mismatched decoding of intersymbol interference using a parallel concatenated scheme,” *IEEE J. Select. Areas Commun.*, vol. 16, no. 2, pp. 255–259, 1998.
  - [10] J.-J. van de Beek, O. Edfors, M. Sandell, S. K. Wilson, and P. O. Börjesson, “On channel estimation in OFDM systems,” in *Proc. IEEE Vehicular Technology Conference (VTC '95)*, pp. 815–819, Chicago, Ill, USA, July 1995.
  - [11] A. Doucet, N. de Freitas, and N. Gordon, *Sequential Monte Carlo in Practice*, Springer-Verlag, New York, NY, USA, 2001.
  - [12] A. Doucet, S. Godsill, and C. Andrieu, “On sequential Monte Carlo sampling methods for Bayesian filtering,” *Statistics and Computing*, vol. 10, no. 3, pp. 197–208, 2000.
  - [13] X. Wang, R. Chen, and J. Liu, “Monte Carlo signal processing for wireless communications,” *Journal of VLSI Signal Processing*, vol. 30, no. 1–3, pp. 89–105, 2002.
  - [14] Z. Yang and X. Wang, “A sequential Monte Carlo blind receiver for OFDM systems in frequency-selective fading channels,” *IEEE Trans. Signal Processing*, vol. 50, no. 2, pp. 271–280, 2002.
  - [15] L. Bahl, J. Cocke, F. Jelinek, and J. Raviv, “Optimal decoding of linear codes for minimizing symbol error rate (Corresp.),” *IEEE Trans. Inform. Theory*, vol. 20, no. 2, pp. 284–287, 1974.



**Dong Guo** received the B.S. degree in geophysics and computer science from China University of Mining and Technology (CUMT), Xuzhou, China, in 1993, and the M.S. degree in geophysics from the Graduate School of Research Institute of Petroleum Exploration and Development (RIPED), Beijing, China, in 1996. In 1999, he received the Ph.D. degree in applied mathematics from Beijing University, Beijing, China. In 2004, he received a second Ph.D. degree in electrical engineering from Columbia University, New York. His research interests are in the area of statistical signal processing and communications.



**Xiaodong Wang** received the B.S. degree in electrical engineering and applied mathematics (with the highest honors) from Shanghai Jiao Tong University, Shanghai, China, in 1992; the M.S. degree in electrical and computer engineering from Purdue University in 1995; and the Ph.D. degree in electrical engineering from Princeton University in 1998. From July 1998 to December 2001, he was on the faculty of the Department of Electrical Engineering, Texas A&M University. In January 2002, he joined the Department of Electrical Engineering, Columbia University. Dr. Wang's research interests fall in the general areas of computing, signal processing, and communications. Among his publications is a recent book entitled *Wireless Communication Systems: Advanced Techniques for Signal Reception*, published by Prentice Hall. Dr. Wang has received the 1999 NSF CAREER Award. He has also received the 2001 IEEE Communications Society and Information Theory Society Joint Paper Award. He currently serves as an Associate Editor for the IEEE Transactions on Signal Processing, the IEEE Transactions on Communications, the IEEE Transactions on Wireless Communications, and IEEE Transactions on Information Theory.

**Zigang Yang** received the B.S. degree in electrical engineering and applied mathematics in 1995, and the M.S. degree in electrical engineering in 1998, both from Shanghai Jiaotong University (SJTU), Shanghai, China. In 2002, she got the Ph.D. degree in electrical engineering from Texas A&M University, College Station, Texas. From 1999 till 2002, she was a Research Assistant with the Department of Electrical Engineering, Texas A&M University. Currently, she is working as a system engineer at Texas Instrument, Communication R&D Lab. Her research interests are in the area of statistical signal processing and its applications, primarily in digital communications.

